High-Resolution Diffusion-Weighted Neuroimaging at 3T and 7T with Simultaneous Multi-Slice RESOLVE

Robert Frost[1]; Peter J. Koopmans[1]; George W. Harston[2]; James Kennedy[2]; Peter Jezzard[1]; Karla L. Miller[1]; David A. Porter[3]

[1] FMRIB Centre, Nuffield Department of Clinical Neurosciences, University of Oxford, Oxford, UK
[2] Radcliffe Department of Medicine, University of Oxford, Oxford, UK
[3] Fraunhofer Institute for Medical Image Computing MEVIS, Bremen, Germany

Introduction

Single-shot echo-planar imaging

Diffusion-weighted imaging is an important tool in both clinical imaging and neuroscience research. Its widespread use is due to the advent of the single-shot echo-planar imaging (ss-EPI) sequence [1], which is relatively immune to motion-related diffusion-encoding artifacts because all the required data for each image are acquired in a single 'shot' after the diffusion encoding. This insensitivity to motion, particularly cardiac-related brain pulsation, and the ability to rapidly acquire a multi-slice volume are the reasons why, 25 years after it was first introduced [2], spin echo ss-EPI remains the most commonly-used diffusion imaging sequence for the assessment of acute stroke [3] and white matter anisotropy [4]. However, ss-EPI suffers from the well-known geometric distortion artifact as well as the more subtle blurring due to T2* decay of the signal. These issues limit the achievable spatial resolution, particularly at high field strengths where increased artifact levels directly undermine the goal of improved spatial resolution.

RESOLVE

One approach to overcoming these limitations is to use diffusion-weighted, readout-segmented EPI (RESOLVE) [5] which is becoming established as an alternative to ss-EPI that provides improved image quality in a wide range of clinical applications throughout the body [6-14].

RESOLVE belongs to a family of sequences that have addressed the ghosting and blurring artifacts that arise in multi-shot diffusion imaging due to phase inconsistencies between the shots. RESOLVE measures the motion-related phase caused by the diffusion encoding in a so-called 'navigator' echo acquired at the centre of *k*-space (see Fig. 1A). The navigator phase information is acquired after every shot of the multi-shot image and is used to correct motion-induced phase errors to generate an artifact-free image [15, 16].

A particular advantage of the readout-segmented approach to multi-shot image acquisition [17] (shown in Fig. 1B) is that an efficient 2D non-linear navigator phase correction [18]

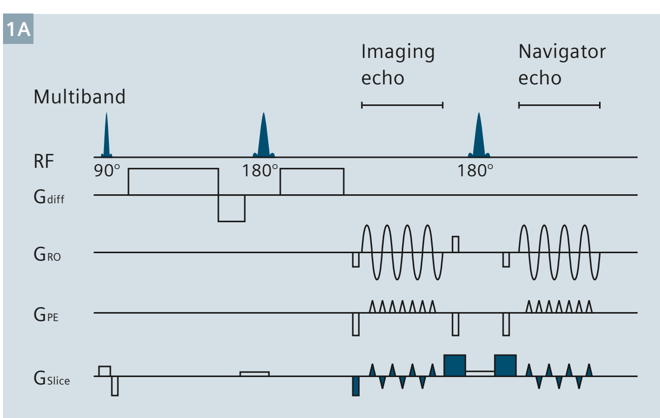

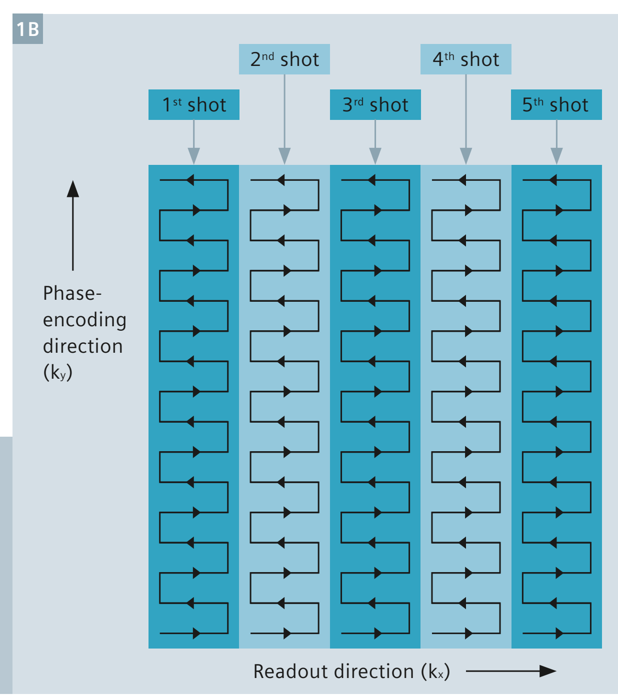

1 **(1A)** Schematic diagram of the RESOLVE sequence. SMS modifications are colored blue.
(1B) A schematic diagram of the RESOLVE *k*-space acquisition for five readout-segments.

can be used because the *k*-space data sampling fulfils the Nyquist condition, which avoids the confounding effects of aliased signal contributions. A related feature of RESOLVE that is necessary for robust diffusion imaging, is a navigator-based selective reacquisition that identifies shots with particularly severe motion-induced phase corruption and reacquires them [19, 20].

The possibility of multi-shot acquisition with RESOLVE reduces sensitivity to distortion and T2* blurring artifacts in comparison to ss-EPI. Images are less distorted because the phase evolution time between adjacent *k*-space lines (echo-spacing) is shorter and T2* blurring is reduced because the total duration of each shot is shorter. Both features are consequences of acquiring sub-sets of *k*-space in multiple shots or repetition times (TRs) rather than encoding the whole of *k*-space in a single shot. This makes it possible to acquire high-spatial-resolution diffusion-weighted images because the sequence avoids the severe limitations seen with ss-EPI, where there is a trade-off between resolution and the level of geometric distortion and blurring.

RESOLVE can also be combined with GRAPPA [21] to further reduce the effective echo-spacing and readout duration [22]. The reduced duration of the EPI readout with RESOLVE compared to ss-EPI also results in a shorter echo time (TE), which reduces signal loss due to T2 decay; this is particularly significant at ultra-high field strengths, such as 7T, due to the shorter T2 decay times.

Simultaneous multi-slice RESOLVE

Acquiring multiple shots to form each image increases the RESOLVE scan time compared to ss-EPI. Techniques to accelerate the sequence are therefore important for routine clinical use and to increase the number of diffusion-weighted directions for diffusion tensor imaging (DTI) or tractography. Two advances that reduce RESOLVE scan times have recently been demonstrated: 1) readout partial Fourier (PF) acquisition [23] and 2) simultaneous multi-slice (SMS) acceleration [24, 25]. These two techniques are compatible and can, in combination, deliver substantial reductions in the RESOLVE scan time, thereby making whole-brain studies with multiple diffusion directions feasible.

At 7T, radiofrequency (RF) heating constraints often lead to extended scan times and this is exacerbated when acquiring multiple slices simultaneously with SMS acceleration, which, in itself, increases the specific absorption rate (SAR). These effects can be mitigated by using low-SAR 'Power Independent of Number of Slices' (PINS) RF pulses [26], which make SMS acceleration possible at 7T. The PINS technique has therefore been combined with SMS RESOLVE to enable 1 mm isotropic DTI at ultra-high field [27].

The recent work described in this article demonstrates how time-efficient, high-resolution SMS RESOLVE[1] images have important advantages over ss-EPI for clinical stroke imaging and for DTI. In addition, the article shows how the combination of PINS and SMS RESOLVE makes it possible to acquire high-resolution, whole-brain DTI at ultra-high field.

SMS RESOLVE

SMS acquires data from multiple slices together and extracts the slice-specific information using a parallel imaging reconstruction [28]. As fewer slice excitations are required to cover the volume, the TR can be reduced, thereby accelerating the scan and increasing the SNR efficiency. A crucial feature of EPI-based SMS is the blipped-CAIPIRINHA modification that improves SNR by reducing the *g*-factor [29] of the reconstruction, which is achieved by imparting differential in-plane shifts of adjacent slices using slice gradients during the EPI readout [30-33].

The SMS modifications to RESOLVE [24, 25] are shown in Figure 1A (colored blue). Data were acquired on a MAGNETOM Verio 3T and an actively-shielded MAGNETOM 7T[2]. Figure 2 shows examples of SMS RESOLVE images with 26 slices acquired at 3T in 2:14 min with a nominal pixel size of 1 × 1 × 5 mm, an SMS acceleration factor (R_{slice}) of 2 and an in-plane GRAPPA acceleration factor (R_{PE}) of 2; single-shot EPI images acquired in 55 s are provided for comparison.

[1] The product is still under development and not commercially available yet. Its future availability cannot be ensured.

[2] MAGNETOM 7T is ongoing research. All data shown are acquired using a non-commercial system under institutional review board permission. MAGNETOM 7T is still under development and not commercially available yet. Its future availability cannot be ensured.

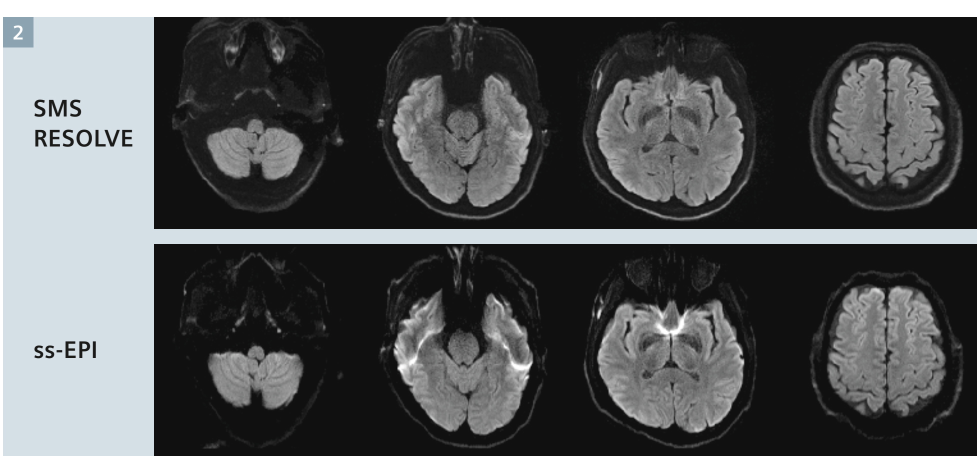

2 Comparison of nominal 1 × 1 × 5 mm resolution trace-weighted images between SMS RESOLVE (top row) and ss-EPI (bottom row) acquired at 3T with 26 slices.

The SMS RESOLVE images show a significant reduction in distortions and T2* blurring compared to the ss-EPI images.

The single-shot EPI images acquired in this study used a routine clinical protocol with a partial Fourier (PF) factor of 6/8 in the phase-encode direction to reduce the echo time (TE) and thereby boost SNR. The images were reconstructed in the standard way using zero-filling (ZF) which creates additional blurring in the phase-encode direction. Despite this blurring, it is standard practice to use ZF with diffusion-weighted ss-EPI because it is more robust than other PF reconstruction algorithms in the presence of motion-induced phase imparted during the diffusion preparation [34].

Comparisons with standard ss-EPI in this study did not use SMS to accelerate the ss-EPI scans. SMS would reduce the scan times and increase the SNR efficiency of the ss-EPI acquisitions, but the image quality, which is the focus of the comparisons, would not be affected.

Clinical stroke imaging with SMS RESOLVE

SMS RESOLVE scans can be a viable clinical alternative to standard ss-EPI DWI for stroke diagnosis, which is typically acquired using an isotropic resolution of around 2 mm. SMS RESOLVE with $R_{slice} = 2$ and $R_{PE} = 2$ can reliably acquire high-quality data at higher resolution with reduced distortion and blurring artifacts. Figure 3 demonstrates the improved image quality provided by SMS RESOLVE with a 1.5 mm isotropic resolution (78 slices) compared to typically-acquired lower-resolution ss-EPI images with $R_{PE} = 2$ and a nominal pixel size of 1.8 × 1.8 × 2 mm with 0.6 mm slice gap (50 slices). The following comparisons (Figs. 4-6) show matched 3:20 min scan times and 1.5 mm isotropic resolution (78 slices) for SMS RESOLVE versus ss-EPI (3 averages) and indicate further potential advantages of using SMS RESOLVE.

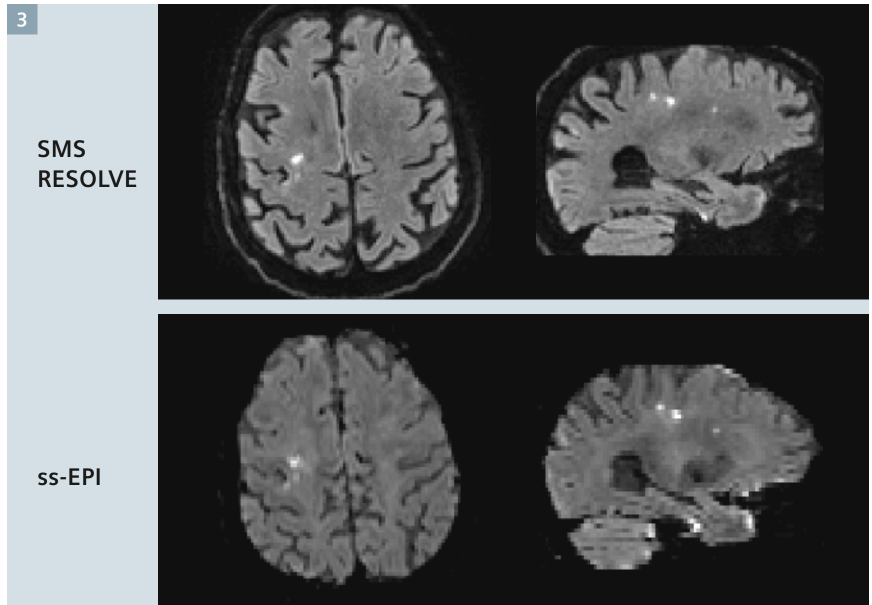

3 Comparison of 1.5 mm isotropic SMS RESOLVE (top row) and 1.8 × 1.8 × 2 mm with 0.6 mm slice gap ss-EPI images (bottom row) acquired at 3T. The images show a right subcortical infarct. The SMS RESOLVE and ss-EPI scans acquired 78 and 50 slices, respectively.

Reduced distortion artifact confounds
SMS RESOLVE has fewer confounding 'signal pile-up' artifacts caused by distortion, in the posterior fossa, brainstem and in proximity to the sinuses, especially the frontal sinus. The improvements are especially apparent in Figures 4 and 5, which show the similarity in appearance of infarcts and signal pile-up artifact in the ss-EPI images. Suppressing these artifacts in the SMS RESOLVE images improves the recognition of regions of true restricted diffusion.

Improved quantification of infarct volume
Previous clinical imaging studies in stroke [10] and of pelvic tumors in radiotherapy planning applications [12] have confirmed that RESOLVE provides an improved geometric distortion performance when compared to ss-EPI; similar benefits are to be expected when SMS RESOLVE images are used to estimate infarct volume in acute stroke. The importance of accurately tracking infarct volume in acute stroke imaging has recently been identified in the Acute Stroke Imaging Research Roadmap II [35]. However, the accuracy of quantifying infarct volume from standard ss-EPI images is limited by the substantial distortion and blurring artifacts. In particular, subtle injuries depicted in Figure 6 are better defined in the SMS RESOLVE images.

7T DTI with PINS SMS RESOLVE

RESOLVE DWI becomes more advantageous at higher resolution because the corresponding ss-EPI acquisitions require an increase in both the echo-spacing and the number of echoes to increase resolution along the readout and phase-encoding axes respectively; this results in a substantial increase in the level of distortion and T2* blurring. These effects become particularly significant at 7T due to amplification of susceptibility and reduced relaxation times. In the case of RESOLVE, the higher resolution in the readout direction is achieved by increasing the number of readout segments, or shots, without a change in echo spacing and only the number of echoes is increased; in this case, there is no increase in distortion at higher resolution and T2* blurring is substantially less than in the ss-EPI case.

However, the technical capability to perform DWI with small voxel sizes and

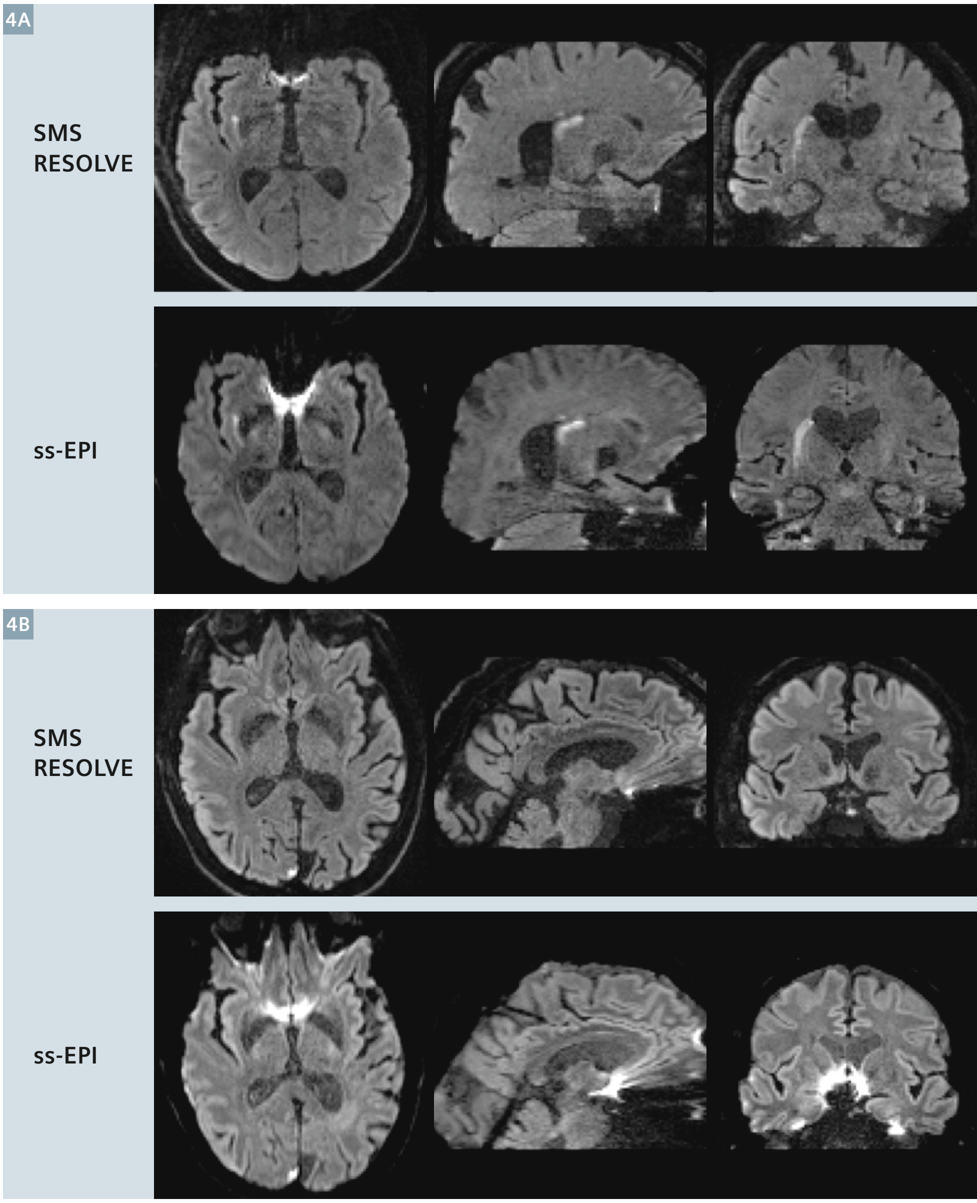

4 Comparison of 1.5 mm isotropic SMS RESOLVE (top row) and ss-EPI images (bottom row) acquired at 3T highlighting the reduction of signal pile up artifact caused by geometric distortions. Panel **(4A)** shows a right lenticulostriate artery infarct and panel **(4B)** shows a right occipital infarct. 78 slices were acquired in both scans.

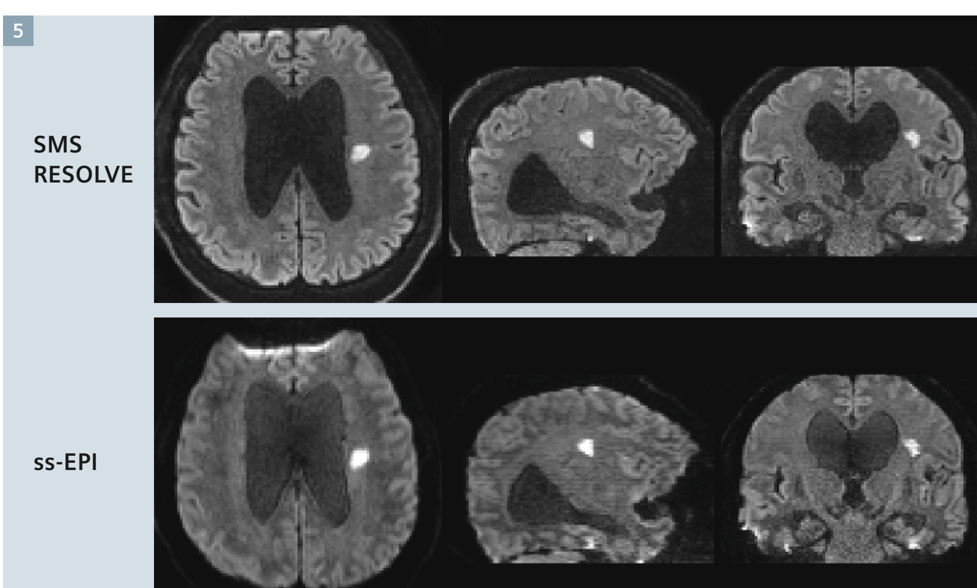

5 Comparison of 1.5 mm isotropic SMS RESOLVE (top row) and ss-EPI images (bottom row) acquired at 3T highlighting the reduction of geometric distortion in proximity to the frontal sinuses. The images show a left lacunar infarct. 78 slices were acquired in both scans.

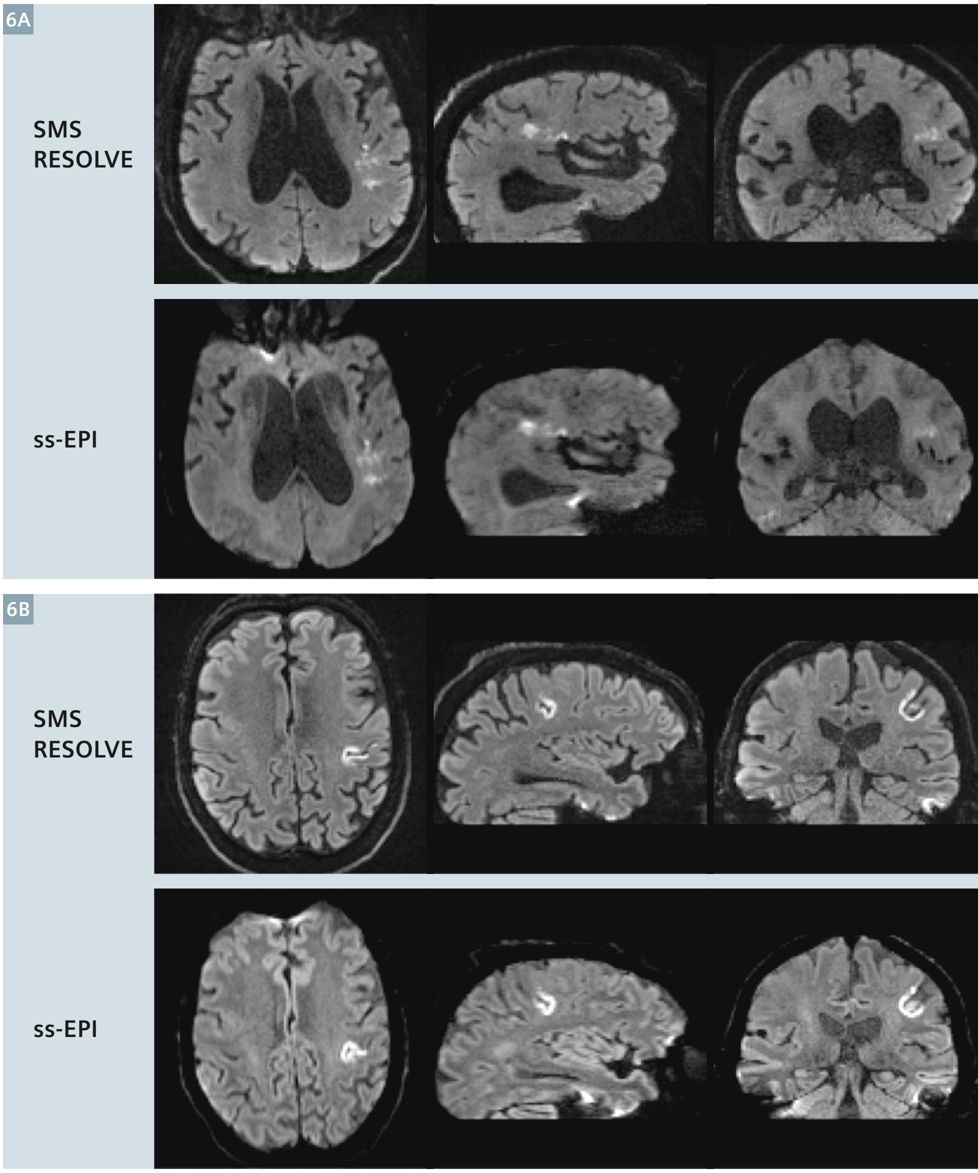

6 Comparison of 1.5 mm isotropic SMS RESOLVE (top row) and ss-EPI images (bottom row) acquired at 3T highlighting the improved depiction of subtle injuries with SMS RESOLVE. Confounding signal pile-up artifacts in the ss-EPI images are also reduced with SMS RESOLVE. Panel **(6A)** shows a left middle cerebral artery territory subcortical infarct and panel **(6B)** shows left middle cerebral artery territory cortical infarcts. 78 slices were acquired in both scans.

a low level of T2* blurring is compromised by the corresponding reduction in SNR, which is already inherently low in DWI due to signal attenuation at high b-value. For isotropic resolution with a small slice thickness, SNR efficiency is further reduced by the requirement to use long TR times to accommodate the increased number of slices. Strategies for increasing SNR and maximising acceleration therefore have an important role to play when using RESOLVE to perform high-resolution DTI.

One way to meet these goals is to perform imaging studies at higher B_0 field strength, where there is increased SNR and improved performance of parallel imaging because the coil sensitivities are more distinct [36]. There are however a number of additional challenges at 7T, including B_0 and RF inhomogeneity, SAR constraints and shorter T2 values than at lower field strengths. The combination of PINS and SMS RESOLVE has the potential to meet these challenges and provide a technique that can exploit the potential benefits of diffusion-weighted imaging at 7T. In particular, the shortened readout time reduces distortion, T2* blurring and the effects of signal loss due to T2 decay, and the low-SAR PINS RF pulses allow high slice-acceleration factors to be used with low TR, resulting in high SNR efficiency.

SMS RESOLVE at 7T

As shown previously in studies without SMS, the RESOLVE acquisition scheme is inherently less sensitive to the very high level of B_0 distortion and T2* blurring that affects ss-EPI at 7T [37]. Figure 7 demonstrates how these benefits can also be seen when the technique is combined with slice acceleration to reduce scan time; the figure compares 1.2 mm isotropic SMS RESOLVE images using $R_{slice} = 3$ and $R_{PE} = 2$ with standard ss-EPI images (also with $R_{PE} = 2$). The SMS RESOLVE scan with 99 slices was acquired with 6 segments (6/7 readout PF), 0.32 ms echo-spacing, 32 b = 1000 s/mm^2 diffusion directions, and with 4 interspersed low-b-value images in 35 min. A consequence of the

7

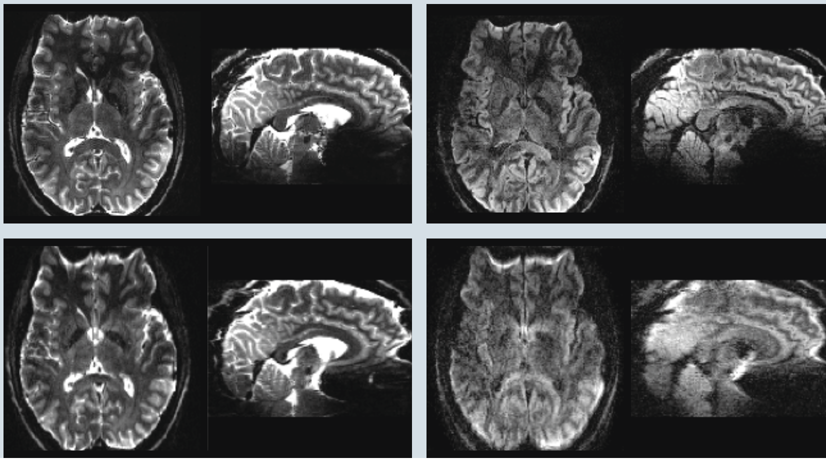

7 Comparison of 1.2 mm isotropic SMS RESOLVE (top row) and ss-EPI images (bottom row) acquired at 7T (99 slices) highlighting the reduction of geometric distortion and blurring with SMS RESOLVE.

8

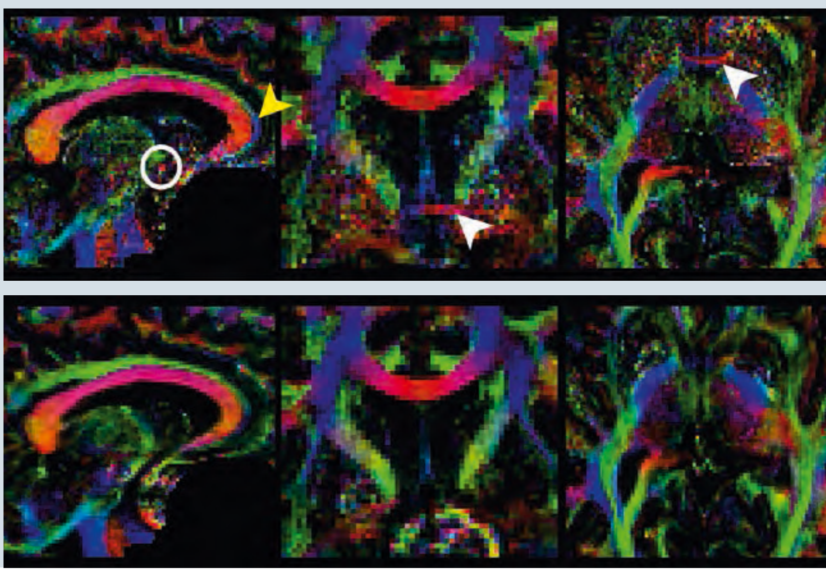

8 7T DTI results comparing blurring and distortion in 1.2 mm isotropic SMS RESOLVE and ss-EPI acquisitions with 99 slices. Color-coded maps of the principal diffusion direction weighted by the fractional anisotropy are shown. The SMS RESOLVE data show the anterior commissure (white circle and arrows), which is not present in the ss-EPI data. SMS RESOLVE also exhibits reduced blurring and distortion in the cingulum (yellow arrow).
Color code:
green, anterior–posterior;
blue, superior–inferior;
red, left–right.

artifact reduction is highlighted in the color-coded principal diffusion direction (PDD) maps weighted by the fractional anisotropy (FA) of Figure 8. The thin anterior commissure tract is missing in the ss-EPI data (in both the matched slice and the surrounding slices) because it is in a region of high distortion but it is clearly visualised in the SMS RESOLVE images. However, in this first proof of principle, the SMS RESOLVE data utilized standard (non-PINS) RF pulses, which resulted in SAR limitations that necessitated an increased TR, and, as such, the ideal 3-fold scan time reduction could not be achieved.

PINS SMS RESOLVE at 7T

PINS RF pulses directly address the SAR restriction that otherwise limits the SMS

9

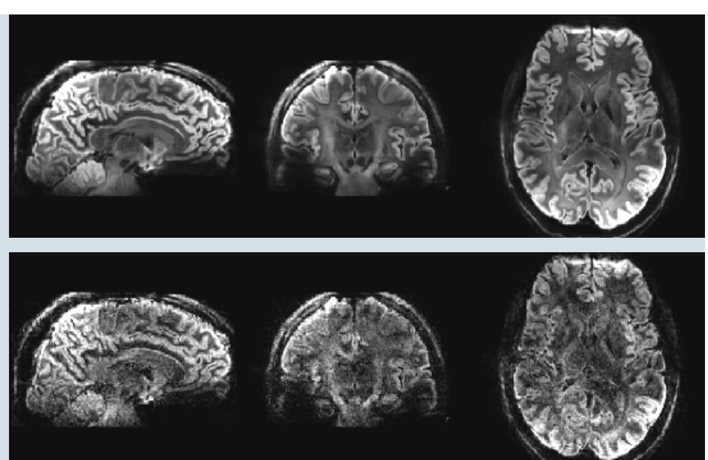

9 1.2 mm isotropic PINS SMS RESOLVE images (99 slices) acquired at 7T with b = 800 s/mm². The mean of 80 diffusion directions (top row) and a single diffusion direction are shown (bottom row).

scan-time reduction that can be realized at 7T. Figure 9 shows 1.2 mm isotropic images with 99 slices acquired using PINS SMS RESOLVE [27] with 80 diffusion-gradient directions and 12 averages with low b-value in a scan time of 38 minutes; the data were acquired without readout partial Fourier using $R_{slice} = 3$, $R_{PE} = 2$, five readout segments, an echo-spacing of 0.38 ms and b = 800 s/mm^2; the figure shows the mean of all the diffusion-weighted images and data from a single diffusion direction. The color-coded PDD FA map in Figure 10 highlights the fine tract resolution and good contrast of these data.

Figure 11 shows data from a PINS SMS RESOLVE scan with 1 mm isotro-

10

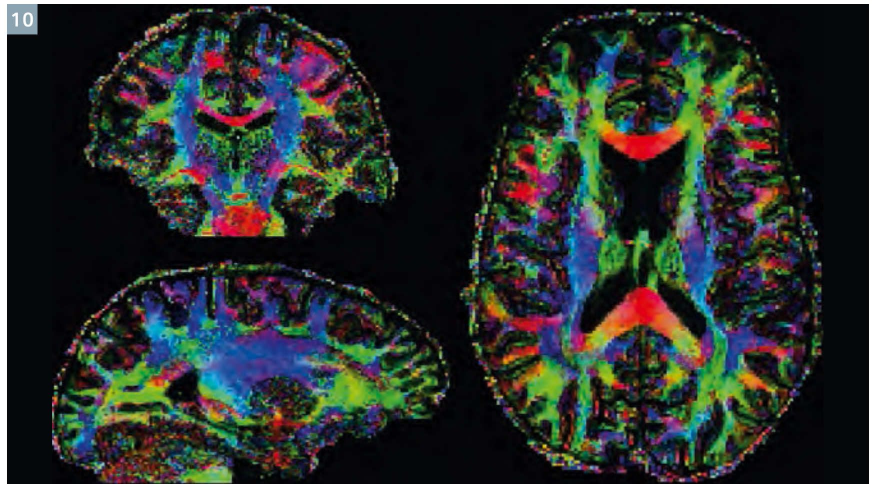

10 7T DTI results of a 1.2 mm isotropic PINS SMS RESOLVE acquisition (99 slices) demonstrating fine resolution and good contrast of the anisotropy. Color-coded maps of the principal diffusion direction weighted by the fractional anisotropy are shown. Color code: green, anterior–posterior; blue, superior–inferior; red, left–right.

11

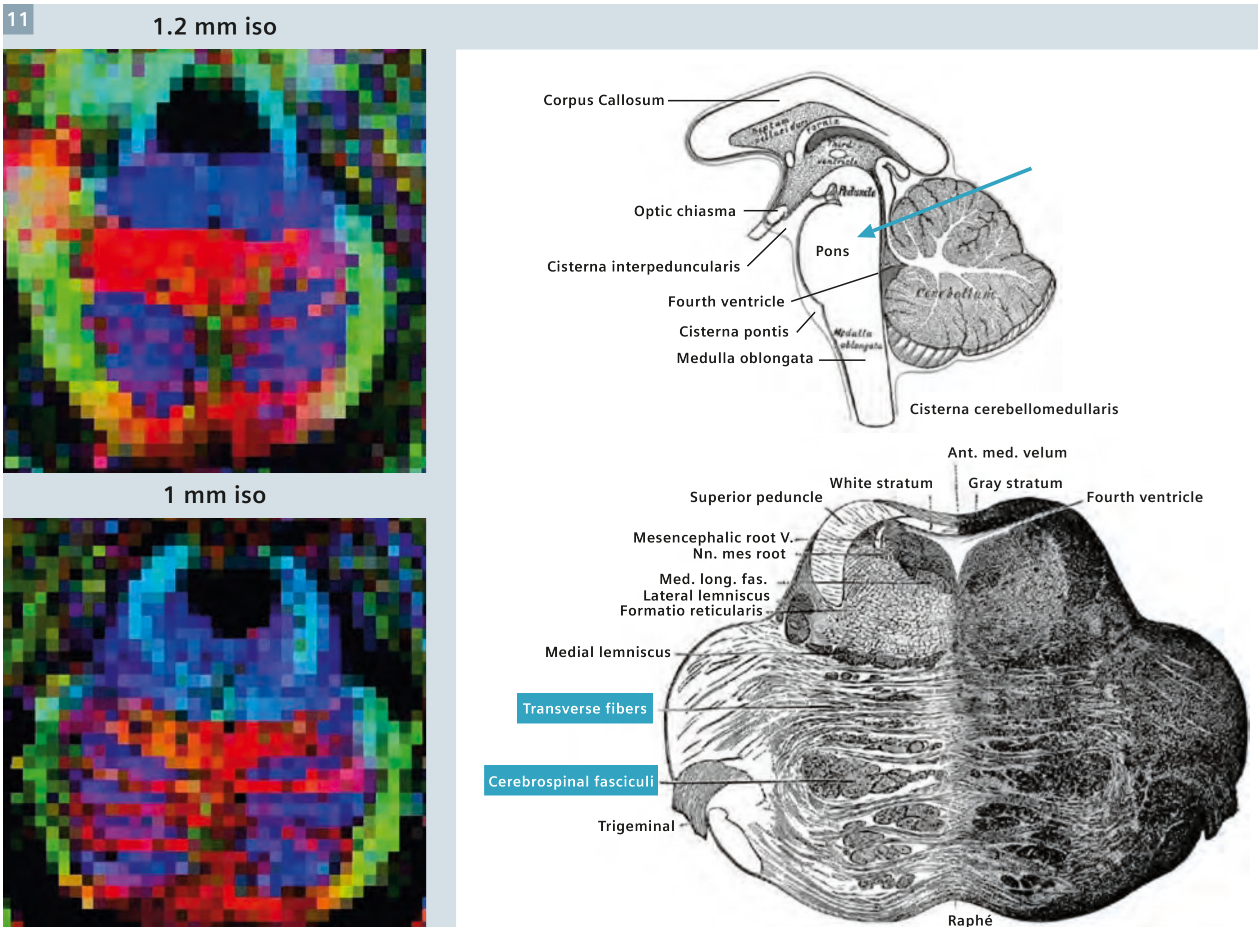

11 7T DTI results comparing 1.2 mm and 1 mm isotropic PINS SMS RESOLVE acquisitions. The thin transverse pontocerebellar fibers are more clearly resolved in the 1 mm isotropic images (in a different healthy volunteer). The transverse pontocerebellar fibers (running right-left, colored red) interdigitate with the cerebrospinal fasciculi (running superior-inferior, colored blue). The 1.2 mm and 1 mm acquisitions acquired 99 and 117 slices, respectively. Color-coded maps of the principal diffusion direction weighted by the fractional anisotropy are shown. Color code: green, anterior–posterior; blue, superior–inferior; red, left–right. *The anatomical drawings are adaped from Gray's Anatomy (1918).*

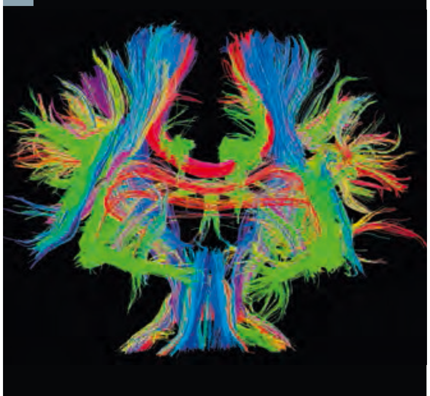

12 7T tractography generated from 1 mm isotropic PINS SMS RESOLVE data with 117 slices. Color code: green, anterior–posterior; blue, superior–inferior; red, left–right.

pic resolution and 117 slices in a scan time of 45 minutes; the images were acquired with $R_{slice} = 3$, $R_{PE} = 2$ using 3 readout segments (3/5 readout PF), an echo spacing of 0.40 ms, 60 scans at b = 580 s/mm^2, 60 scans at b = 1160 s/mm^2 and 13 scans with low b-value. This, in comparison with the 1.2 mm isotropic data suggests potential advantages of high-resolution DTI by showing improved depiction (in a different subject) of the transverse pontocerebellar fibers (running right-left) that interdigitate with the cerebrospinal fasciculi (running superior-inferior). An example of whole-brain tractography with the 1 mm isotropic data is shown in Figure 12. This image was generated using the Diffusion Toolkit and TrackVis [38].

In summary, PINS RF pulses make it possible to acquire high-resolution RESOLVE at 7T with a slice-acceleration factor of three; this enables acquisition protocols with a large number of diffusion directions and multiple b-value shells with acquisition times that are acceptable for neuroscientific applications. Data sets of this type provide valuable input for advanced tractography analyses that probe secondary fiber populations. The preliminary results acquired with the technique suggest that the SMS RESOLVE sequence could become a powerful tool for *in vivo* tractography of fine structure.

Other applications of SMS RESOLVE

In addition to the brain imaging applications reported in this paper, preliminary work reported elsewhere has shown that SMS RESOLVE can provide data for combined tractography studies of the brain and cervical spine [39]. Studies of this type are not possible with ss-EPI due to the high level of susceptibility-based distortion around the spinal cord. The SMS RESOLVE technique has also been applied to diffusion-weighted breast imaging of healthy volunteers, demonstrating acquisitions with reduced acquisition times with potential application in clinical studies of breast tumors [40], where the standard RESOLVE technique has been shown to provide a clinical benefit [8].

As an alternative to the SMS RESOLVE technique described in this paper, a simultaneous, multi-slab acquisition method has also been proposed, in which a 3D-encoded version of the RESOLVE sequence [41] is used to simultaneously encode data in multiple slabs [42].

Conclusion

The results shown in this paper demonstrate that SMS RESOLVE makes it possible to perform diffusion-weighted imaging of the whole brain with isotropic resolution and shortened scan times that are suitable for clinical stroke protocols. The improved image quality compared to ss-EPI provides a clearer depiction of infarcts with fewer confounding susceptibility artifacts and the reduction in geometrical distortion is expected to provide a more accurate quantification of lesion volume.

This paper has also shown how the SMS RESOLVE technique can be combined with PINS RF pulses to exploit slice-acceleration at 7T without the constraints of high SAR, making it possible to acquire high-quality data sets for advanced tractography studies which require a large number of diffusion-gradient directions. The technique also promises to enhance clinical diffusion-weighted imaging at 7T, for which preliminary studies with the standard RESOLVE technique are producing promising results [43].

SMS RESOLVE is an appealing alternative to standard ss-EPI DWI with potential benefits for clinical and scientific applications in the brain and other organs. The clinical benefit of the standard RESOLVE technique has been established in a large number of studies, but there is typically an acquisition-time penalty relative to lower-quality image acquisitions with ss-EPI. This limitation is much less prohibitive when RESOLVE is combined with SMS and readout PF to accelerate the scans and this combination increases the potential of the technique to substantially improve the quality of diffusion-weighted imaging in a wide variety of applications.

Acknowledgements

We thank the NIHR Oxford Biomedical Research Centre and the Medical Research Council for funding. PK acknowledges funding by the Wellcome Trust [WT100092MA]. We are also grateful for funding to the NIHR Clinical Research Network, the Dunhill Medical Trust [grant number: OSRP1/1006] and the Centre of Excellence for Personalized Healthcare funded by the Wellcome Trust and Engineering and Physical Sciences Research Council [grant number: WT088877/Z/09/Z]. We thank Thorsten Feiweier of Siemens Healthcare for the diffusion preparation module used in this work. We also thank Juliet Semple and Peter Manley for assistance with data acquisition and are grateful for the facilities provided by the Oxford Acute Vascular Imaging Centre (AVIC).

References

1 Mansfield P, Pykett IL. Biological and medical imaging by NMR Journal of Magnetic Resonance (1969) 1978;29:355–373.
2 Turner R, Le Bihan D, Maier J, Vavrek R, Hedges LK, Pekar J. Echo-planar imaging of intravoxel incoherent motion. Radiology 1990;177:407–414.
3 Warach S, Gaa J, Siewert B, Wielopolski P, Edelman RR. Acute human stroke studied by whole brain echo planar diffusion-weighted magnetic resonance imaging. Ann Neurol 1995;37:231–241.
4 Basser PJ, Mattiello J, LeBihan D.

Estimation of the effective self-diffusion tensor from the NMR spin echo. J Magn Reson B 1994;103:247–254.
5 Porter DA, Heidemann RM. High resolution diffusion-weighted imaging using readout-segmented echo-planar imaging, parallel imaging and a two-dimensional navigator-based reacquisition. Magn Reson Med 2009;62:468–475.
6 Hayes LL, Jones RA, Palasis S, Aguilera D, Porter DA. Drop metastases to the pediatric spine revealed with diffusion-weighted MR imaging. Pediatr Radiol 2012;42:1009–1013.
7 Rumpel H, Chong Y, Porter DA, Chan LL. Benign versus metastatic vertebral compression fractures: combined diffusion-weighted MRI and MR spectroscopy aids differentiation. Eur Radiol 2013;23:541–550.
8 Bogner W, Pinker-Domenig K, Bickel H, Chmelik M, Weber M, Helbich TH, Trattnig S, Gruber S. Readout-segmented Echo-planar Imaging Improves the Diagnostic Performance of Diffusion-weighted MR Breast Examinations at 3.0 T Radiology 2012;263:64–76.
9 Wisner DJ, Rogers N, Deshpande VS, Newitt DN, Laub GA, Porter DA, Kornak J, Joe BN, Hylton NM. High-resolution diffusion-weighted imaging for the separation of benign from malignant BI-RADS 4/5 lesions found on breast MRI at 3T Journal of Magnetic Resonance Imaging 2014;40:674–681.
10 Morelli J, Porter D, Ai F, Gerdes C, Saettele M, Feiweier T, Padua A, Dix J, Marra M, Rangaswamy R, Runge V. Clinical evaluation of single-shot and readout-segmented diffusion-weighted imaging in stroke patients at 3 T. Acta Radiol 2013;54:299–306.
11 Thian YL, Xie W, Porter DA, Weileng Ang B. Readout-segmented echo-planar imaging for diffusion-weighted imaging in the pelvis at 3T-A feasibility study. Acad Radiol 2014;21:531–537.
12 Foltz WD, Porter DA, Simeonov A, Aleong A, Jaffray D, Chung P, Han K, Ménard C. Readout-segmented echo-planar diffusion-weighted imaging improves geometric performance for image-guided radiation therapy of pelvic tumors Radiotherapy and Oncology.
13 Tokoro H, Fujinaga Y, Ohya A, Ueda K, Shiobara A, Kitou Y, Ueda H, Kadoya M. Usefulness of free-breathing readout-segmented echo-planar imaging (RESOLVE) for detection of malignant liver tumors: comparison with single-shot echo-planar imaging (SS-EPI). Eur J Radiol 2014;83:1728–1733.
14 Friedli I, Crowe LA, Viallon M, Porter DA, Martin P, de Seigneux S, Vallee J. Improvement of renal diffusion-weighted magnetic resonance imaging with readout-segmented echo-planar imaging at 3T. Magn Reson Imaging 2015;33:701–708.
15 Ordidge RJ, Helpern JA, Qing ZX, Knight RA, Nagesh V. Correction of motional artifacts in diffusion-weighted MR images using navigator echoes. Magn Reson Imaging 1994;12:455–460.
16 Anderson AW, Gore JC. Analysis and correction of motion artifacts in diffusion weighted imaging. Magn Reson Med 1994;32:379–387.
17 Robson MD, Anderson AW, Gore JC. Diffusion-weighted multiple shot echo planar imaging of humans without navigation. Magn Reson Med 1997;38:82–88.
18 Miller KL, Pauly JM. Nonlinear phase correction for navigated diffusion imaging. Magn Reson Med 2003;50:343–353.
19 Nguyen Q, Clemence M, Ordidge RJ. The use of intelligent re-acquisition to reduce scan time in MRI degraded by motion. In: Proceedings of the 6th Annual Meeting of ISMRM, 1998 (abstract 134).
20 Porter DA. 2D-navigator-based re-acquisition for motion artefact suppression in multi-shot, diffusion-weighted imaging. In: Proceedings of the 14th Annual Meeting of ISMRM, 2006 (abstract 1047).
21 Griswold MA, Jakob PM, Heidemann RM, Nittka M, Jellus V, Wang J, Kiefer B, Haase A. Generalized autocalibrating partially parallel acquisitions (GRAPPA). Magn Reson Med 2002;47:1202–1210.
22 Porter DA, Heidemann RM. Multi-shot, diffusion-weighted imaging at 3T using readout-segmented EPI and GRAPPA In: Proceedings of the 14th Annual Meeting of ISMRM, Seattle, Washington, USA, 2006 (abstract 1046).
23 Frost R, Porter DA, Miller KL, Jezzard P. Implementation and assessment of diffusion-weighted partial Fourier readout-segmented echo-planar imaging. Magn Reson Med 2012;68:441–451.
24 Frost R, Porter DA, Douaud G, Jezzard P, Miller KL. Reduction of diffusion-weighted readout-segmented EPI scan time using a blipped-CAIPI modification. In: Proceedings of the 20th Annual Meeting of ISMRM, 2012 (abstract 116).
25 Frost R, Jezzard P, Douaud G, Clare S, Porter DA, Miller KL. Scan time reduction for readout-segmented EPI using simultaneous multislice acceleration: Diffusion-weighted imaging at 3 and 7 tesla. Magn Reson Med 2015;74:136–149.
26 Norris DG, Koopmans PJ, Boyacioglu R, Barth M. Power Independent of Number of Slices (PINS) radiofrequency pulses for low-power simultaneous multislice excitation. Magn Reson Med 2011;66:1234–1240.
27 Koopmans PJ, Frost R, Porter DA, Wu W, Jezzard P, Miller KL, Barth M. Diffusion-weighted readout-segmented EPI using PINS simultaneous multislice imaging. In: Proceedings of the 23rd Annual Meeting of ISMRM, 2015 (abstract 959).
28 Larkman DJ, Hajnal JV, Herlihy AH, Coutts GA, Young IR, Ehnholm G. Use of multicoil arrays for separation of signal from multiple slices simultaneously excited. J Magn Reson Imaging 2001;13:313–317.
29 Pruessmann KP, Weiger M, Scheidegger MB, Boesiger P. SENSE: sensitivity encoding for fast MRI. Magn Reson Med 1999;42:952–962.
30 Breuer FA, Blaimer M, Heidemann RM, Mueller MF, Griswold MA, Jakob PM. Controlled aliasing in parallel imaging results in higher acceleration (CAIPIRINHA) for multi-slice imaging. Magn Reson Med 2005;53:684–691.
31 Nunes RG, Hajnal JV, Golay X, Larkman DJ. Simultaneous slice excitation and reconstruction for single shot EPI. In: Proceedings of the 14th Annual Meeting of ISMRM, 2006 (abstract 293).
32 Setsompop K, Cohen-Adad JA, McNab JA, Gagoski B, Wedeen VJ, Wald LL. Improving SNR per unit time in diffusion Imaging using a blipped-CAIPIRINHA simultaneous multi-slice EPI acquisition. In: Proceedings of the 18th Annual Meeting of ISMRM, 2010 (abstract 187).
33 Setsompop K, Gagoski BA, Polimeni JR, Witzel T, Wedeen VJ, Wald LL. Blipped-controlled aliasing in parallel imaging for simultaneous multislice echo planar imaging with reduced g-factor penalty. Magn Reson Med 2012;67:1210–1224.
34 Robson MD, Porter DA. Reconstruction as a source of artifact in non-gated single-shot diffusion-weighted EPI. Magn Reson Imaging 2005;23:899–905.
35 Wintermark M, Albers GW, Broderick JP, Demchuk AM, Fiebach JB, Fiehler J, Grotta JC, Houser G, Jovin TG, Lees KR, Lev MH, Liebeskind DS, Luby M, Muir KW, Parsons MW, von Kummer R, Wardlaw JM, Wu O, Yoo AJ, Alexandrov AV, Alger JR, Aviv RI, Bammer R, Baron J, Calamante F, Campbell BCV, Carpenter TC, Christensen S, Copen WA, Derdeyn CP, Haley ECJ, Khatri P, Kudo K, Lansberg MG, Latour LL, Lee T, Leigh R, Lin W, Lyden P, Mair G, Menon BK, Michel P, Mikulik R, Nogueira RG, Ostergaard L, Pedraza S, Riedel CH, Rowley HA, Sanelli PC, Sasaki M, Saver JL, Schaefer PW, Schellinger PD, Tsivgoulis G, Wechsler LR, White PM, Zaharchuk G, Zaidat OO, Davis SM, Donnan GA, Furlan AJ, Hacke W, Kang D, Kidwell C, Thijs VN, Thomalla G, Warach SJ. Acute Stroke Imaging Research Roadmap II. Stroke 2013;44:2628–2639.
36 Wiesinger F, Van de Moortele P, Adriany G, De Zanche N, Ugurbil K, Pruessmann KP. Potential and feasibility of parallel MRI at high field NMR in Biomedicine 2006;19:368–378.
37 Heidemann RM, Porter DA, Anwander A, Feiweier T, Heberlein K, Knosche TR, Turner R. Diffusion imaging in humans at 7T using readout-segmented EPI and

GRAPPA. Magn Reson Med 2010;64:9–14.
38 Wang R, Benner T, Sorensen AG, Wedeen VJ. Diffusion Toolkit: a software package for diffusion imaging data processing and tractography. In: Proceedings of the 15th Annual Meeting of ISMRM, 2007 (abstract 3720).
39 Liu W, Bhat H, Cohen-Adad J, Setsompop K, Wang D, Beck T, Cauley SF, Zhou K, Porter DA. Large-FOV tractography of the brain and spinal cord with reduced scan time: a study using diffusion-weighted readout-segmented EPI and simultaneous multi-slice acceleration In: Proceedings of the 23rd Annual Meeting of ISMRM, 2015 (abstract 4434).
40 Liu W, Bhat H, Weiland E, Wang D, Beck T, Cauley SF, Porter DA. Readout-segmented EPI with simultaneous, multi-slice acceleration for the rapid acquisition of high-resolution, diffusion-weighted images of the breast In: Proceedings of the 23rd Annual Meeting of ISMRM, 2015 (abstract 1605).
41 Frost R, Miller KL, Tijssen RHN, Porter DA, Jezzard P. 3D Multi-slab diffusion-weighted readout-segmented EPI with real-time cardiac-reordered k-space acquisition. Magn Reson Med 2014;72:1565–1579.
42 Frost R, Jezzard P, Porter DA, Tijssen RHN, Miller KL. Simultaneous multi-slab acquisition in 3D multi-slab diffusion-weighted readout-segmented echo-planar imaging. In: Proceedings of the 21st Annual Meeting of ISMRM, 2013 (abstract 3176).
43 Bogner W, Pinker K, Zaric O, Baltzer P, Minarikova L, Porter D, Bago-Horvath Z, Dubsky P, Helbich TH, Trattnig S, Gruber S. Bilateral diffusion-weighted MR imaging of breast tumors with submillimeter resolution using readout-segmented echo-planar imaging at 7 T. Radiology 2015;274:74–84.

Contact

Dr. Robert Frost
FMRIB Centre
John Radcliffe Hospital
Oxford OX3 9DU
UK
robert.frost@ndcn.ox.ac.uk

Learn more!

Don’t miss the talks of experienced and renowned experts on all aspects of MR imaging at:

www.siemens.com/magnetom-world